J Mol Model (2004) 10:76–84
DOI 10.1007/s00894-003-0174-5

ORIGINAL PAPER

Karmen Voda · Bojana Boh · Margareta Vrtačnik

A quantitative structure–antifungal activity relationship study of oxygenated aromatic essential oil compounds using data structuring and PLS regression analysis

Received: 4 May 2003 / Accepted: 14 November 2003 / Published online: 20 December 2003

Abstract Twenty two oxygenated aromatic essential oil compounds were chosen for the study of the antifungal activity against two wood-decaying fungi, the white-rot *Trametes versicolor*, which mainly metabolizes lignin, and the brown-rot *Coniophoha puteana*, which digests cellulose in plant cell walls. Minimal inhibitory concentrations (MICs) were determined by the agar dilution method, using dimethyl sulfoxide (DMSO) as the solvent for the selected compounds and potato-dextrose agar (PDA) as the growth medium for both fungi. The MICs were then used to generate a tree structure, which represents the structuring of the essential oil compounds by the nature and position of the substituents in their aromatic rings, and as dependent variables (log(1/MIC)) in the QSAR analysis. Data structuring proved that a relationship between the molecular structures of the essential oil compounds and their antifungal activity exists, and the hypotheses derived therefrom were complemented by performing a QSAR analysis using the partial least squares (PLS) method. Statistically significant PLS models were obtained with the 1-octanol–water partition coefficient (*C* log *P*), the energy of the highest occupied molecular orbital (E_{HOMO}), and the number of hydrogen-bond donor atoms in the molecules of the compounds studied (Donor) for *T. versicolor* and with *C* log *P* and the fractional negative surface area (FNSA1) for *C. puteana*.

Keywords QSAR · Oxygenated aromatic compounds · Essential oils · Antifungal activity · Wood-degrading fungi

K. Voda (✉) · B. Boh · M. Vrtačnik
Department of Chemical Education and Informatics,
Faculty of Natural Sciences and Engineering,
University of Ljubljana,
Vegova 4, 1000 Ljubljana, Slovenia
e-mail: karmen.voda@uni-lj.si
Tel.: +386-1-251-4326
Fax: +386-1-425-8486

Introduction

Essential oils have a long history as traditional medicinal agents. Phenols (thymol, carvacrol, eugenol) and other oxygenated aromatic essential-oil compounds such as phenol ethers (*trans*-anethole, methyl chavicol) and aromatic aldehydes (cinnamaldehyde, cuminaldehyde) have been reported to exert both antibacterial [1] and antifungal activity, [2] and are thus constantly being investigated for possibilities of application in food preserving and as natural antimicrobial agents in human and veterinary medicine [3, 4, 5, 6, 7, 8].

The white-rot *Trametes versicolor* and the brown-rot *Coniophora puteana*, both members of the basidiomycetes family, cause the degradation of lignin and cellulose in wood. Besides other enzymes, *T. versicolor* produces extracellular laccase, a blue multi-copper oxidoreductase, which catalyzes the oxidation of phenolic species to phenoxy radicals, which may further be prone to enzymatic oxidation reactions to form quinones, or to non-enzymatic reactions such as hydration and polymerization [9, 10, 11]. *C. puteana* on the other hand, produces extracellular cellobiose dehydrogenase (CDH), which plays an important role in the initial stages of brown-rot wood decay by catalyzing the oxidation of cellodextrins, mannodextrins, and lactose in hemicellulose to their corresponding lactones. The oxidation reaction is coupled with the reduction of a wide spectrum of electron acceptors including quinones and phenoxy radicals [12, 13]. This phenomena occurs through the Fenton reaction (Fe(II)-oxalate+H_2O_2→Fe(III)-oxalate+$OH^{\cdot}$+OH^{-}), which yields free hydroxyl radicals, which subsequently form pores in the enveloping hemicellulose and thus allow the diffusion of cellulases and their action upon cellulose microfibrils in plant cell walls [14,15].

Many QSAR studies on the biological action of phenols have been reported. Acute phenolic toxicity on tadpoles was investigated by Wang and co-workers, [16] on algae by Lu and co-workers, [17] and their cytotoxic action on rat liver cells by Hansch and co-workers [18]. QSARs describing phenolic antioxidant properties, [19]

skin irritant potentials [20] and antibacterial activity towards oral bacteria [21, 22] have also been reported. A common finding of most QSAR studies dealing with the investigation of a biological activity of a set of compounds in vivo is the descriptive importance of the macroscopic hydrophobicity descriptor log *P*, which represents the ability of a compound to penetrate the cell membrane and reach the interacting sites [16, 23]. In bioreactions, where binding to another atom and electron-transfer reactions such as oxidation and reduction are involved, E_{HOMO} and E_{LUMO}, as the quantum chemical descriptors associated with the ionization potential and electronic affinity of a molecule, have also proven to yield good correlations [17, 24]. Geban and co-workers [25] discovered that the electron density of the highest occupied molecular orbital at the sulfur and oxygen atoms of 3,4-disubstituted-1,2,4-oxa(thia)-diazole-5(4 H)-ones(thiones) is strongly related to their antibacterial and antifungal activity as these sites are the key sites for binding to mercapto (–SH) groups in enzyme active sites, which is the basis of their antimicrobial activity. Similarly, the antifungal action of phenols is based on the inhibition of fungal enzymes containing –SH groups in their active sites [26] and the *T. versicolor* laccase is an example of such an enzyme.

The application of essential oils or their chemical constituents in wood preservation has not yet been reported. The purpose of our study was to correlate the experimentally determined antifungal activity of 22 essential oil phenols, phenol ethers, and aromatic aldehydes towards the white-rot *T. versicolor* and the brown-rot *C. puteana* with structural features of the molecules of the selected compounds and thus explore the possibilities of application of essential oils as natural preservatives in wood preservation formulations against these two wood-decaying fungi. Since the target fungal enzymes of the inhibitory action of phenolic compounds towards *T. versicolor* and *C. puteana* have not yet been identified, a further goal of the QSAR analysis was to gain more information on the biomechanism of the selected compounds' inhibitory action in order to gain information on the possible structure of the target enzymes' active sites and infer on their nature.

Structure–activity relationships were first investigated by structuring data into a tree structure and the hypotheses derived therefrom were complemented with the results obtained by performing PLS-QSAR with hydrophobicity, quantum chemical, structural, and geometrical molecular descriptors.

Materials and methods

Chemicals

Phenol and hydroquinone were purchased from Riedel de Haen, Germany, benzaldehyde and DMSO from Kemika Zagreb, Croatia, and anisaldehyde from Merck, Germany. Thymol was a courtesy of Krka Pharmaceuticals Novo Mesto, Slovenia, and vanillin and ethyl vanillin were a courtesy of Aero Celje, Chemical, Graphic and Paper Industry, Slovenia. All the other chemicals were purchased from Aldrich, Germany.

Antifungal activity assay

Minimal inhibitory concentrations (MICs) of 22 essential-oil phenols, phenol ethers and aromatic aldehydes (Table 1) for the brown-rot *Trametes versicolor* (ZIM L053) and the white-rot *Coniophora puteana* (ZIM L010) were determined with a screening test by the agar dilution method. DMSO was used as the solvent for the selected essential-oil compounds (nine concentrations between 2×10^{-2} mol l^{-1} and 7.8×10^{-5} mol l^{-1} were tested) and potato-dextrose agar (PDA) as the growth medium for both wood-degrading fungi [27, 28]. Fungi growing on PDA alone and on PDA with an addition of DMSO represented the controls and every experiment was performed in triplicate. MICs of the compounds tested were labeled as the concentrations, which, after 1 week of incubation at 25 °C and 75% relative humidity in a growth chamber, prevented any visible growth of the fungi or any other visible changes, such as staining of the growth medium, which would indicate a reaction of the fungi towards the inhibitory compounds. In the cases of hydroquinone, *o*-cresol, guaiacol, and coniferaldehyde, MICs greater than 0.02 mol l^{-1} could not be determined because the preparation of such high concentrations was not possible.

Data structuring

Based on the experimentally determined MIC values, a tree structure was constructed (Fig. 1) using methods for structuring data into systems, [29] which represents the structuring of the selected oxygenated aromatic essential oil compounds by the nature and position of their substituents in the aromatic ring. Structural formulae of the compounds tested were arranged into a tree structure in the following way: branching in the first level was achieved by considering the nature of the substituent in the first position of the aromatic ring R_1, which was either a hydroxyl, a methoxy, or an aldehyde group. If two of these groups were present in the molecule, e.g. an –OH and an –OMe group, the molecule was treated as a phenol (R_1=–OH), because literature references dealing with the antifungal activity of phenols on the two chosen wood-degrading fungi are quite large in number, while those dealing with the antifungal activity of phenol ethers and aromatic aldehydes on the two wood-degrading fungi were not found. The resulting three subgroups were subsequently structured according to the compounds' substituents in the second position of the aromatic ring (R_2=–H, –Me, –*i*-Pr, –OMe, –OEt, –COOMe), followed by the third (R_3=–H, –Me, –*i*-Pr), fourth (R_4=–H, –Me, –*i*-Pr, *cis*- and *trans*-1-propenyl, 2-propenyl, –OH, –CHO,

Table 1 Selected essential oil phenols, phenol ethers, and aromatic aldehydes, tested for their antifungal activity against *T. versicolor* and *C. puteana*

Compound 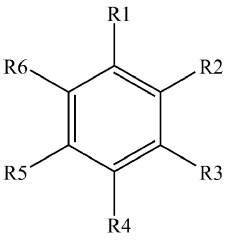	R_1	R_2	R_3	R_4	R_5	R_6
Phenol	*-OH*	*-H*	*-H*	*-H*	*-H*	*-H*
o-Cresol	*-OH*	*-CH_3*	*-H*	*-H*	*-H*	*-H*
m-Cresol	*-OH*	*-H*	*-CH_3*	*-H*	*-H*	*-H*
p-Cresol	*-OH*	*-H*	*-H*	*-CH_3*	*-H*	*-H*
Thymol	*-OH*	*-i-Pr*	*-H*	*-H*	*-CH_3*	*-H*
Carvacrol	*-OH*	*-H*	*-i-Pr*	*-H*	*-H*	*-CH_3*
Creosol	*-OH*	*-OCH_3*	*-H*	*-CH_3*	*-H*	*-H*
Isoeugenol	*-OH*	*-OCH_3*	*-H*	*-cis-, trans-1-propenyl*	*-H*	*-H*
Eugenol	*-OH*	*-OCH_3*	*-H*	*-2-propenyl*	*-H*	*-H*
Coniferaldehyde	*-OH*	*-OCH_3*	*-H*	*-propenal*	*-H*	*-H*
Hydroquinone	*-OH*	*-H*	*-H*	*-OH*	*-H*	*-H*
Vanillin[a]	*-OH*	*-OCH_3*	*-H*	*-CHO*	*-H*	*-H*
Ethyl vanillin[a]	*-OH*	*-OCH_2CH_3*	*-H*	*-CHO*	*-H*	*-H*
Guaiacol	*-OH*	*-OCH_3*	*-H*	*-H*	*-H*	*-H*
Methyl salycilate	*-OH*	*-$COOCH_3$*	*-H*	*-H*	*-H*	*-H*
trans-Anethole	*-OCH_3*	*-H*	*-H*	*-trans-1-propenyl*	*-H*	*-H*
Methyl eugenol	*-OCH_3*	*-OCH_3* [18]	*-H*	*-2-propenyl*	*-H*	*-H*
Methyl chavicol	*-OCH_3*	*-H*	*-H*	*-2-propenyl*	*-H*	*-H*
p-Methoxy phenylacetone	*-OCH_3*	*-H*	*-H*	*-ketopropyl*	*-H*	*-H*
Benzaldehyde	*-CHO*	*-H*	*-H*	*-H*	*-H*	*-H*
Anisaldehyde	*-CHO*	*-H*	*-H*	*-OCH_3*	*-H*	*-H*
Cuminaldehyde	*-CHO*	*-H*	*-H*	*-i-Pr*	*-H*	*-H*

[a]Vanillin and ethyl vanillin are found in ethanolic vanilla bean extracts (*Vanilla plantifolia, V. tahitensis, and V. pompona*). [8]

–CH=CH–CHO, 2-ketopropyl), fifth (R_5=–H, –Me) and sixth position of the aromatic ring (R_6=–H, –Me). The resulting branches of the tree structure were then linked to the experimentally determined MICs and potential structure–activity patterns were sought. By identifying the most active and least active compounds in the tree structure, the substituent or substituents, which may be the potential reason for a compound's antifungal activity, were searched for by moving from the right to the left side of the tree structure and comparing the substituents in the same positions of the aromatic ring.

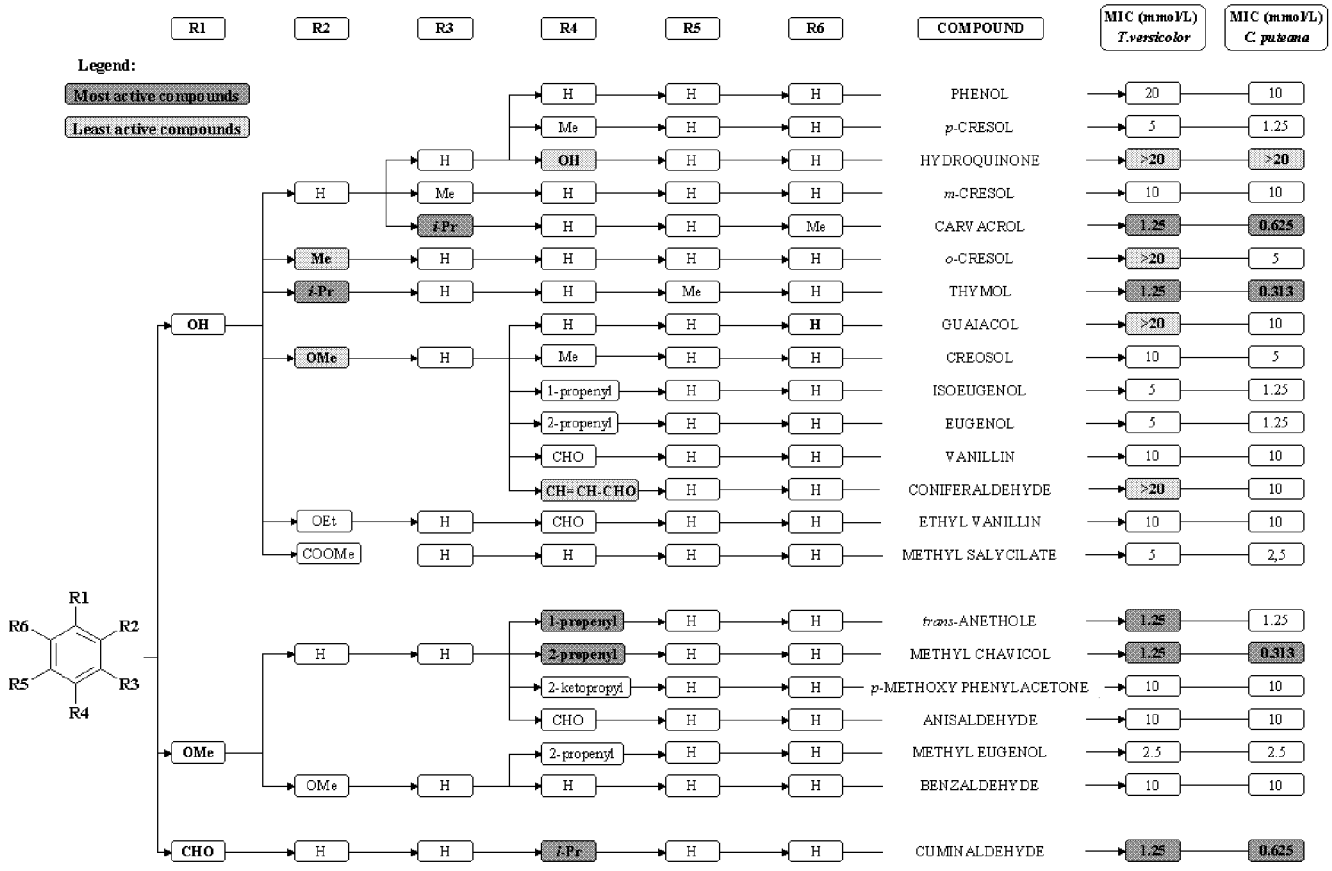

Fig. 1 Tree structure representing the structuring of the oxygenated aromatic essential-oil compounds by the position and nature of their substituents in the aromatic ring

Calculation of molecular descriptors and PLS-QSAR analysis

Two assumptions were made prior to the PLS-QSAR analysis: (1) MICs of compounds that were experimentally determined to be greater than 0.02 mol l^{-1} were assumed to be 0.1 mol l^{-1} (log(1/MIC)=1) to enable the inclusion of these compounds in the PLS analysis and (2) the isomeric mixture of *cis*- and *trans*-isoeugenol was treated as *trans*-isoeugenol because the 1-propenyl, 2-propenyl, and 1-propenal chains in the fourth position of the aromatic ring of structurally similar compounds in the data set (eugenol, *trans*-anethole, methyl chavicol, methyl eugenol, and coniferaldehyde) all have *trans*-conformations. *C* log *P* was calculated with the Tetko and coworkers' [30] Java-based software and molar refractivity (CMR) was calculated with PCModels, [31] both available on the Internet. Calculations of all other molecular descriptors and PLS-QSAR analyses were performed with SYBYL 6.7.2 [32] on a Silicon Graphics Workstation (IRIX 6.5 operating system). Full geometry optimization of the molecular structures and calculations of E_{HOMO} and E_{LUMO} were carried out with the AM1 Hamiltonian using MOPAC 6.0, implemented in SYBYL. The resulting PLS regression equations were checked for validity by the "leave-one-out" cross-validation method, while the best PLS-QSAR models were additionally evaluated with the PRESS (predictive residual sum of squares), PRESS/SS_y (SS_y is the sum of squares of the dependent variable *Y*–log(1/MIC) values) and *s*/ΔAct. (ratio of the standard error of estimate and the experimentally determined antifungal activity range) statistical parameters for the evaluation of QSAR models.

Results

The results of the experimental determination of MICs for the 22 essential-oil compounds revealed thymol, carvacrol, *trans*-anethole, methyl chavicol, and cuminaldehyde as the antifungally most active compounds (MIC=1.25×10^{-3} mol l^{-1}), while hydroquinone, *o*-cresol, guaiacol, and coniferaldehyde were the least active compounds against *T. versicolor* (MIC >0.02 mol l^{-1}). Similarly, thymol, carvacrol, *trans*-anethole, and cuminaldehyde exhibited the greatest inhibitory action (MIC=6.25×10^{-4} and 3.13×10^{-4} mol l^{-1}), while hydroquinone was the least active compound against *C. puteana* (MIC > 0.02 mol l^{-1}). The MICs are presented

Table 2 Experimentally determined antifungal activity values and calculated molecular descriptors for the 22 oxygenated aromatic essential oil compounds

Compound	log(1/MIC) (*T.v.*)	log(1/MIC) (*C.p.*)	*C* log *P*	E_{HOMO} (eV)	E_{LUMO} (eV)
Phenol	1.699	2.000	1.48	–9.114074	0.398342
o-Cresol	1.000	2.301	1.92	–8.998954	0.368562
m-Cresol	2.000	2.000	1.97	–9.025227	0.393198
p-Cresol	2.301	2.903	1.97	–8.884176	0.426914
Thymol	2.903	3.505	3.20	–8.946260	0.369294
Carvacrol	2.903	3.204	3.35	–8.900223	0.368714
Creosol	2.000	2.301	1.82	–8.634310	0.420392
trans-Isoeugenol[a]	2.301	2.903	2.45	–8.420338	0.005979
Eugenol	2.301	2.903	2.40	–8.662725	0.392749
Coniferaldehyde	1.000	2.000	1.23	–8.850618	–0.799590
Hydroquinone	1.000	1.000	0.81	–8.735112	0.231246
Vanillin	2.000	2.000	1.28	–9.127688	–0.475626
Ethyl vanillin	2.000	2.000	1.81	–9.094283	–0.452038
Guaiacol	1.000	2.000	1.32	–8.969929	0.264306
Methyl salycilate	2.301	2.602	2.34	–9.388046	–0.497670
trans-Anethole	2.903	3.505	3.31	–8.775615	0.196881
Methyl eugenol	2.602	2.602	2.87	–9.142030	0.190911
Methyl chavicol	2.903	2.903	3.13	–8.816012	0.492724
p-Methoxy phenylacetone	2.000	2.000	1.35	–9.030088	0.232234
Benzaldehyde	2.000	2.000	1.50	–10.002219	–0.433860
Anisaldehyde	2.000	2.000	1.78	–9.369038	–0.376464
Cuminaldehyde	2.903	3.204	2.92	–9.752234	–0.457878
cis-Isoeugenol[a]	2.301	2.903	2.58	–8.520932	0.131259

Compound	Electronegativity (eV)	Donor	Acceptor	FNSA1	CMR
Phenol	4.357866	1	1	0.255	2.8417
o-Cresol	4.315196	1	1	0.386	3.3055
m-Cresol	4.316014	1	1	0.472	3.3055
p-Cresol	4.228631	1	1	0.438	3.3055
Thymol	4.288483	1	1	0.730	4.6969
Carvacrol	4.265754	1	1	0.610	4.6969
Creosol	4.106959	1	2	0.557	3.9224
trans-Isoeugenol[a]	4.207180	1	2	0.518	4.9006
Eugenol	4.134988	1	2	0.275	4.8246
Coniferaldehyde	4.825104	1	3	0.411	5.1643
Hydroquinone	4.251933	2	2	0.289	2.9948
Vanillin	4.801657	1	3	0.413	3.9581
Ethyl vanillin	4.773160	1	3	0.340	4.4219
Guaiacol	4.352811	1	2	0.372	3.4586
Methyl salycilate	4.942858	1	3	0.398	3.9581
trans-Anethole	4.289367	0	1	0.513	4.7475
Methyl eugenol	4.475559	0	2	0.302	5.2884
Methyl chavicol	4.161644	0	1	0.256	4.6715
p-Methoxy phenylacetone	4.398927	0	2	0.329	4.7326
Benzaldehyde	5.218040	0	1	0.295	3.1881
Anisaldehyde	4.872751	0	2	0.379	3.8050
Cuminaldehyde	5.105056	0	1	0.543	4.5795
cis-Isoeugenol[a]	4.194837	1	2	0.172	4.9006

[a] Isomeric mixture

in Table 2 as log(1/MIC) values which were used as the dependent variables in the PLS-QSAR analysis.

Fig. 1 shows the tree structure, which was constructed by structuring the 22 essential-oil phenols, phenol ethers, and aromatic aldehydes by the nature and position of the substituents in the aromatic ring.

All calculated molecular descriptors are presented in Table 2. E_{HOMO} and E_{LUMO} are the energies of the highest occupied and lowest unoccupied molecular orbitals, FNSA1 (fractional negative surface area 1) is the ratio between the partial negative surface area and the total surface area of the molecules (Eq. 1), Donor and Acceptor represent the number of hydrogen bond donor and acceptor atoms in the molecules, and MR is the molar refractivity. *N* (relative hardness) and electronegativity were calculated with Eqs. (2) and (3) [20].

$$\text{FNSA1} = \Sigma(-A_i)/A_{\text{total}} \quad \text{(Eq.1)}$$

$-A_i$=area of the *i*th negative atomA_{total}=total molecular surface area

$$N = \tfrac{1}{2}(E_{\text{LUMO}} - E_{\text{HOMO}}) \quad \text{(Eq.2)}$$

$$\text{Electronegativity} = -\tfrac{1}{2}(E_{\text{HOMO}} + E_{\text{LUMO}}) \quad \text{(Eq.3)}$$

The construction of the best PLS models describing the antifungal activity of the essential-oil compounds towards

Table 3 Resulting PLS models for the white-rot *Trametes versicolor* and the brown-rot *Coniophora puteana* (Eqs. 4–10)

$\log(1/\mathrm{MIC}) = aC\log P + bE_{\mathrm{HOMO}} + c\mathrm{Donor} + d$								
a	*b*	*c*	*d*	n^a	q^2	r^2	*s*	
Trametes versicolor								
0.730	–	–	0.559	22	0.701	0.745	0.327	(Eq. 4)
0.741	–0.283	–	–2.019	22	0.727	0.769	0.325	(Eq. 5)
0.664	–	–0.231	0.864	22	0.730	0.778	0.319	(Eq. 6)
0.572	–	–0.178	1.130	19	0.883	0.929	0.143	(Eq. 7)
0.633	–0.196	–	0.899	19	0.876	0.914	0.157	(Eq. 8)
$\log(1/\mathrm{MIC}) = aC\log P + b\mathrm{FNSA1} + c$								
a	*b*	*c*		n^a	q^2	r^2	*s*	
Coniophora puteana								
0.749	–	0.873		22	0.794	0.834	0.261	(Eq. 9)
0.677	0.900	1.553		22	0.813	0.859	0.247	(Eq. 10)

[a] *n* is the number of compounds included in the PLS analysis

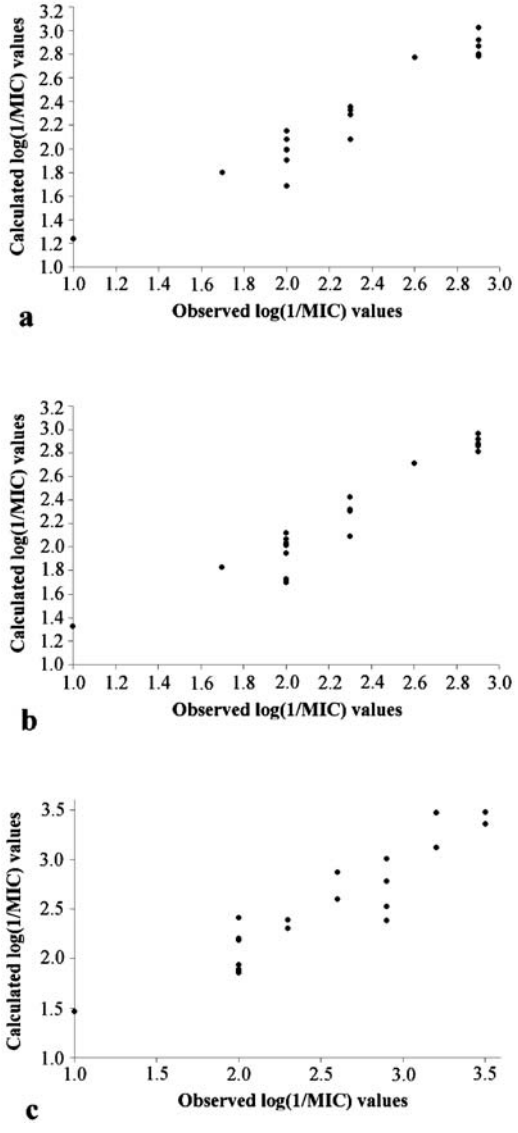

Fig. 2 Relationships between the observed and calculated log(1/MIC) values for the best PLS models: **a** the log *P*–Donor model (Eq. 7), **b** the log *P*–E_{HOMO} model (Eq. 8), (**c**) the log *P*–FNSA1 model (Eq. 10)

the white-rot *T. versicolor* and the brown-rot *C. puteana* is shown in Table 3 (Eqs. 4–10), where *n* represents the number of compounds included in the PLS analysis, q^2 and r^2, respectively, are the cross-validated and non-cross-validated correlation coefficients, and *s* is the standard error of estimate. The observed versus calculated log(1/MIC) values for the best PLS models (Eqs. 7, 8, and 10) are shown in Fig. 2.

Discussion

Knobloch and co-workers [33] reported that among the factors influencing the antifungal activity of essential oil compounds are their hydrophobic properties, which both determine their ability to penetrate the hitin cell walls of fungal hyphae. The most antifungally active compounds against *T. versicolor* and *C. puteana* (thymol, carvacrol, *trans*-anethole, methyl chavicol, and cuminaldehyde) are also the most hydrophobic compounds in the data set with calculated *C* log *P* values ranging from 3.35 for carvacrol and 2.92 for cuminaldehyde, while the least active compounds (*o*-cresol, hydroquinone, guaiacol, and coniferaldehyde) are also the least hydrophobic in the data set with calculated log *P* values ranging from 0.81 for hydroquinone to 1.92 for *o*-cresol, proving the hydrophobicity of compounds to be an important factor for their antifungal activity.

After identifying the structural elements in the generated tree structure (Fig. 1), which were common to the antifungally most active and least active compounds for both types of wood-decaying fungi, the following four hypotheses were derived:

1. Compounds with two or three oxygen-containing groups exhibit a weaker antifungal activity against both of the fungi tested than compounds with only one oxygen-containing group in the aromatic ring.
2. Substituents in the second position of the aromatic ring (e.g. the R_2 –Me and –MeO groups in the cases of *o*-cresol and guaiacol) decrease the antifungal activity of

a compound. In the case of thymol, the *i*-Pr group in the second position is an exception, rendering it one of the most active inhibitory compounds. This is probably the result of stereochemical enhancement encountered during the binding of thymol into the fungal enzyme's active site.

3. Oxygen-containing groups in the fourth position of the aromatic ring (e.g. the R_4 –OH group and the –CHO group at the end of a three-carbon chain in the cases of hydroquinone and coniferaldehyde) decrease the antifungal activity of a compound in comparison with compounds that carry an alkyl or alkenyl group in the same position, e.g. *trans*-anethole, methyl chavicol, and cuminaldehyde.
4. Compounds with oxygen-containing groups in the second and fourth positions of the aromatic ring (vanillin, ethyl vanillin, and coniferaldehyde) are less active than compounds with oxygen-containing groups in the second position and hydrocarbon groups in the fourth position of the aromatic ring (creosol, eugenol, isoeugenol (isomeric mixture), and methyl eugenol). The size of the hydrocarbon group also influences the antifungal activity, where it is evident that compounds with larger groups (*cis*-, *trans*-1-propenyl and 2-propenyl) are antifungally more active than compounds with smaller hydrocarbon groups (–Me).

Before proceeding to the actual PLS-QSAR analysis, relationships between the independent and dependent variables were explored by generating scatter plots, which revealed *C* log *P* as a strong molecular descriptor for the modeling of the experimentally determined MICs for *T. versicolor* and *C. puteana*. The initial *C* log *P*–PLS (Eqs. 4 and 9) model was improved by adding the descriptors in Table 2 to the PLS analysis. The best models for *T. versicolor* were obtained with *C* log *P*, E_{HOMO}, and the number of donor atoms in the molecular structures of the compounds selected (Eqs. 5 and 6), while other descriptors did not yield significant correlations in combination with *C* log *P*. The outliers of Eq. (6) were *o*-cresol, guaiacol, and coniferaldehyde. High residual values between the observed and calculated antifungal activity for these compounds might be the result of the assumption that was made prior to the start of the QSAR analysis—their MICs were experimentally determined to be greater than 0.02 mol l^{-1} and were thus assumed to be 0.1 mol l^{-1} to enable their inclusion in the analysis. They were thus omitted from the PLS analysis, generating the final regression Eqs. (7) and (8). Equation (7) (the *C* log *P*–Donor model) suggests that the higher the calculated *C* log *P* value of a compound and the fewer donor atoms its molecule contains, the greater its antifungal activity. The relative contribution of the *C* log *P* component in the final regression equation was 78.7% and 21.3% for the Donor component.

Donor atoms are the oxygen atoms belonging to hydroxyl groups and may be oxidized to oxygen radicals in enzymatic oxidation reactions such as those catalyzed by the *T. versicolor* laccase. Hydroquinone is the least hydrophobic molecule in the data set and the only compound with two donor atoms in its molecule. Both facts explain hydroquinone's lack of antifungal activity within the concentration range tested. *Trans*-anethole on the other hand, contains a methoxy instead of a hydroxyl group in the first position of the aromatic ring as the only oxygen-containing group in the molecule and thus carries no donor atoms. It is also the second most hydrophobic molecule in the data set according to the calculated *C* log *P* values, which explains its high antifungal activity against *T. versicolor*.

Sakurada and co-workers [24] discovered that the oxidation rate of monosubstituted phenols with horseradish peroxidase correlate well with the quantum chemical descriptor E_{HOMO}. Since the *T. versicolor* laccase oxidizes phenolic compounds to their corresponding phenoxy radicals, a model describing the 19 compounds which yielded the best correlation with *C* log *P* and the number of donor atoms in the molecules of the tested essential oil components, was also constructed with *C* log *P* and E_{HOMO} (Eq. 8). The *C* log *P*–E_{HOMO} model described the structure–antifungal activity relationship of the compounds in the reduced data set almost as well as the *C* log *P*–Donor model, suggesting that the compounds with lower E_{HOMO} values are less prone to enzymatic oxidation and thus exhibit a greater antifungal activity.

The bioactivity of a chemical compound depends on two factors, (1) the transport of the molecule from the outer aqueous medium to a specific target molecule in the biophase of the test organism and (2) the reactivity of the chemical towards the target molecule [34]. The fact that *C* log *P* explains about 80% of the variance in the data set (Eqs. 7 and 8) suggests that the key step in the antifungal activity of the compounds tested towards *T. versicolor* is in reaching the inside of the fungal cells, where they can act upon the fungal enzymes. Hydrophobicity is considered to be largely due to the free energy change associated with the desolvation of a compound as it moves from an aqueous phase to the biological phase with which it interacts to produce biological activity. Log *P* is thus a key factor in transport through a membrane, but it can also control hydrophobic binding to a receptor. If the coefficient is between 0.9 and 1.0, log *P* represents a purely transport term. On the other hand, if the coefficient is about 0.5, log *P* represents a binding term. All the coefficients in the equations in Table 3 are between 0.57 and 0.75 which suggests that log *P* in our case might be modeling both transport and binding. Since Donor and E_{HOMO} represent the remaining 20% of the variance, it can be concluded that enzymatic oxidation reactions play an important role in the mechanism of the antifungal activity of the tested compounds, possibly as competing reactions to the binding of the inhibitors to the –SH groups of cystein residues in the fungal enzymes' active sites, that potentially inactivate phenolic inhibitors such as in the case of the *T. versicolor* laccase. Peroxidases such as lignin peroxidase and manganese peroxidase, which are also produced by *T. versicolor* and have been proven to oxidize phenolic compounds to their corre-

Table 4 Statistical parameters for the evaluation of the three best PLS models

PLS model	n	q^2	s_{CV}	r^2	s	No. of PCs	PRESS	PRESS/SS_y	s/ΔAct. (%)
[a] *C* log *P*–Donor	19	0.883	0.185	0.929	0.143	2	1.023	0.117	7.5
[a] *C* log *P*–E_{HOMO}	19	0.876	0.194	0.914	0.157	2	1.085	0.124	8.3
[b] *C* log *P*–FNSA1	22	0.813	0,284	0.859	0.247	2	1.538	0.187	9.8

[a] PLS model for the white-rot *T. versicolor*
[b] PLS model for the brown-rot *C. puteana*

sponding phenoxy radicals as well, [35,36] could also be the potential targets of phenolic inhibition but limited knowledge of the structures of their substrate-binding active sites prevents further speculation in this direction.

The *C* log *P*–log(1/MIC) scatter plot for *C. puteana* showed three to four linear relationships between the essential-oil compounds in the data set, suggesting possible multiple mechanisms of activities of the compounds, [37, 38] but due to the small number of compounds in the data set, this hypothesis could not be statistically proven. The correlation obtained by using *C* log *P* as the only descriptor in the regression equation was thus improved by gradually including other descriptors from Table 2 in the PLS analysis. Besides *C* log *P*, FNSA1 also proved to be an informative descriptor in correlating the experimentally determined MICs for *C. puteana* with the structural features of the data set. The *C* log *P*–FNSA1 model (Eq. 10) suggests that the higher the calculated *C* log *P* value of a molecule and the higher the ratio between the partial negative surface area and the total surface area of the molecule, the greater the antifungal activity of a compound. The relative contribution of the *C* log *P* component in the final regression equation explains 76.7% of the variance in the data set, while the FNSA1 component explains only 23.3% of the variance, suggesting that the key step in the antifungal activity of the tested compounds, as in the case of *T. versicolor*, is in reaching the inside of the fungal cells, where they can exhibit their inhibitory action upon the fungal enzymes.

Charged partial surface area (CPSA) descriptors such as FNSA1 are used to quantify polar interactions between molecules and represent various combinations of solvent-accessible surface area information and partial atomic charge information, which takes into account both σ and π charges [39]. The FNSA1 value depends on the size of the molecules and the chemical nature of the substituents in the aromatic ring. Ester and aldehyde groups direct π-electrons to *meta*-positions in the aromatic ring, while alkyl, alkenyl, hydroxyl, and alkoxy groups direct π-electrons to *ortho*- and *para*-positions. Electron translations within the aromatic ring and the total electron distribution of the molecule both affect the sum of surfaces of negatively charged atoms (Eq. 1). The most antifungally active compounds for *C. puteana* (thymol, carvacrol, *trans*-anethole, and cuminaldehyde) all contain only one oxygen atom in their molecules and have the highest FNSA1 values (the FNSA1 value for creosol is higher than that of *trans*-anethole, but its greater hydrophilic character renders it less active towards *C. puteana*). The greater the ratio between the negatively charged partial surface area and the whole surface area of the molecules, the more easily the selected compounds might interact with –SH groups in the enzyme active sites and thus exhibit their inhibitory action. Since quantum chemical descriptors such as E_{HOMO} and E_{LUMO} did not improve the initial *C* log *P* regression equation, potential enzymatic oxidations and reductions as competing reactions to the inhibitory action of the selected essential-oil compounds may be excluded. The good correlation obtained with the FNSA1 geometrical descriptor also leads to questions about the structural features of the target fungal enzymes' active sites, which have not yet been identified for phenolic inhibitors in the case of *C. puteana* as well. Since high values of the ratio between the negatively charged partial surface area and the whole surface area of the molecules are favored for their antifungal activity, this might imply that the target fungal enzymes' active sites contain amino acid residues with polar side chains (lysine, arginine, and hystidine), enabling enhanced polar interactions and thus stronger enzyme–inhibitor complexes.

According to the calculated values of the statistical parameters used for the evaluation of the regression equations obtained (Table 4), the best PLS models generated in the PLS-QSAR analysis are all statistically significant. The three best PLS models (Eqs. 7, 8 and 10) yielded good correlations between the experimentally determined log(1/MIC) values for both wood-degrading fungi and the molecular descriptors of compounds included in the regression analyses (r^2>0.85, s<0.24). The "leave-one-out" cross-validation method resulted in high q^2 values (q^2>0.81), representing good predictive ability of the models as well. Both PRESS and PRESS/SS_y are additional criteria used to evaluate the predictive ability of a QSAR model. Models having PRESS/SS_y ratios lower than 0.4 are considered to be statistically significant and predict better than chance, while models having PRESS/SS_y ratios less than 0.1 are excellent [40]. The ratio between the standard error of estimate of the QSAR model and the range of the experimentally determined biological activity (s/ΔAct.) is another criterion for the evaluation of QSAR models and, if determined to be less than 10%, represents statistically good QSAR models [41].

Conclusions

The results of the PLS-QSAR analysis for the modeling of the antifungal activity of the essential-oil compounds tested against both wood-degrading fungi coincide well with the first and roughly with the third and fourth hypotheses derived from data structuring, suggesting that data structuring is a good starting point in SAR studies and the hypotheses derived therefrom may be further studied in-depth by QSAR methods. Conformation of the second and the structural aspects of the third and fourth hypotheses in this stage of the analysis is not yet possible, because size and shape descriptors for substituents in the second and fourth positions of the aromatic ring were not included in the PLS-QSAR analysis. The PLS models obtained provide good correlations for the modeling of the antifungal activity against both wood-degrading fungi. Although it is not known which fungal enzymes are the primary targets of the inhibitory action of the selected compounds, the PLS models obtained provide some insight into the molecular basis of their antifungal activity. To gain a more in-depth understanding of the relationship between the molecular structure and antifungal activity of the selected oxygenated aromatic essential oil compounds, other QSAR methods such as comparative molecular field analysis (CoMFA) and hologram QSAR (HQSAR) will be applied as they enable the introduction of steric, electronic and topological molecular features into the regression equations.

Acknowledgements The authors would like to thank Prof. Dr. Franc Pohleven and Andreja Klinar of the Department of Wood Science and Technology, Biotechnical Faculty, University of Ljubljana, Slovenija for their help and cooperation during the experimental part of this study. Our sincere thanks also goes to Tripos, Inc. (Germany) for allowing us the use of SYBYL 6.7.2 for a time-limited evaluation period. The research was co-founded by the Slovene Ministry of Education, Science and Sport.

References

1. Didry N, Dubreuil L, Pinkas M (1994) Pharm Acta Helv 69:25–28
2. Scora KM, Scora RW (1998) J Basic Microbiol 38:405–413
3. Ettayebi K, El Yamani J, Rossi-Hassani BD (2000) FEMS Microbiol Lett 183:191–195
4. Ultee A, Kets EPW, Smid EJ (1999) Appl Environ Microbiol 65:4606–4610
5. Helander IM, Alakomi HL, Latva-Kala K, Mattila-Sandholm T, Pol I, Smid EJ, Gorris LGM, von Wright A (1998) J Agric Food Chem 46:3590–3595
6. Kim J, Marshall MR, Wei C (1995) J Agric Food Chem 43:2839–2845
7. Zemek J, Valent M, Pódová M, Košíková B, Joniak D (1987) Folia Microbiol 32:421–425
8. Boonchird C, Flegel TW (1982) Can J Microbiol 28:1235–1241
9. Majcherczyk A, Johannes C, Hüttermann A (1999) Appl Microbiol Biotechnol 51:267–276
10. Jolivalt C, Raynal A, Caminade E, Kokel B, Le Goffic F, Mougin C (1999) Appl Microbiol Biotechnol 51:676–681
11. Johannes C, Majcherczyk A, Hüttermann A (1998) J Biotechnol 61:151–156
12. Henriksson G, Johansson G, Pettersson G (2000) J Biotechnol 78:93–113
13. Green III F, Highley TL (1997) Int Biodeterior Biodegrad 39:113–124
14. Hyde SM, Wood PM (1997) Microbiol – UK 143:259–266
15. Ander P (1994) FEMS Microbiol Rev 13:297–312
16. Wang X, Dong Y, Wang L, Han S (2001) Chemosphere 44:447–455
17. Lu GH, Yuan X, Zhao YH (2001) Chemosphere 44:437–440
18. Hansch C, McKarns SC, Smith CJ, Doolittle DJ (2000) Chem–Biol Interact 127:61–72
19. Lien EJ, Ren S, Bui HH, Wang R (1999) Free Rad Biol Med 26:285–294
20. Hayashi M, Nakamura Y, Higashi K, Kato H, Kishida F, Kaneko H (1999) Toxicol in Vitro 13:915–922
21. Shapiro S, Guggenheim B (1998) Quant Struct–Act Relat 17:327–337
22. Shapiro S, Guggenheim B (1998) Quant Struct–Act Relat 17:338–347
23. Dearden JC (1985) Environ Health Perspect 61:203–228
24. Sakurada J, Sekiguti R, Sato K, Hosoya T (1990) Biochemistry 29:4093–4098
25. Geban Ö, Ertepinar H, Yurtsever M, Özden S, Gümüs F (1999) Eur J Med Chem 34:753–758
26. Cowan MM (1999) Clin Microbiol Rev 12:564–582
27. Brock TD, Madigan MT, Martinko JM, Parker J (1994) Biology of microorganisms. Prentice-Hall, Engelwood Cliffs, N.J., p 909
28. Voda K, Boh B, Vrtačnik M, Pohleven F (2003) Int Biodeterior Biodegrad 51:51-59
29. Kornhauser A, Boh B (1992) Information support for research and development in biotechnological applications. In: DaSilva EJ, Ratledge C, Sasson A (eds) Biotechnology: economic and social aspects. Cambidge University Press, Cambridge, pp 309–353
30. Tetko IV, Tanchuk VY, Kasheva TN, Villa AEP (2001) J Chem Inf Comput Sci 41:246–252
31. PCModels—CLOGP 4.72 and CMR 4.71 [online] (2001) Daylight Chemical Information Systems Inc. Available on the internet:http://www.daylight.com/jj-cgi/pcmodels.cgi
32. SYBYL 6.7.2 (2001) Tripos Inc, 1699 South Hanley Rd, St Louis, MO 63144, USA
33. Knobloch K, Pauli A, Iberl B, Weignd H, Weis N (1989) J Essential Oil Res 1:119–128
34. Hansch C, Fujita T (1964) J Am Chem Soc 86:1616–1626
35. Mester T, Tien M (2000) Int Biodeterior Biodegrad 46:51–59
36. Cullen D (1997) J Biotechnol 53:273–289
37. Bearden AP, Schultz TW (1997) Environ Toxicol Chem 16:1311–1217
38. Schultz TW, Holcombe GW, Phipps GL (1986) Ecotoxicol Environ Safety 12:146–153
39. Stanton DT, Jurs PC (1990) Anal Chem 62:2323–2329
40. Clementi S, Wold S (1995) How to choose the proper statistical method? In: van de Waterbeemd H (ed) Chemometric methods in molecular design. VCH, Weinheim, pp 319–338
41. Tong W, Lowis DR, Perkins R, Chen Y, Welsh WJ, Goddette DW, Heritage TW, Sheenan DM (1998) J Chem Inf Comput Sci 38:669–677